Published in : Food Chemistry (2023), vol. 405, Part B, 134927
DOI: 10.1016/j.foodchem.2022.134927
Status : Postprint (Author's version)

MODIFYING SUCROSE ESTERS OLEOGELS PROPERTIES USING DIFFERENT STRUCTURATION ROUTES

Thais Lomonaco Teodoro da Silva [a,*], Vincent Baeten [b], Sabine Danthine [a]

[a]*Science des Aliments et Formulation, Gembloux Agro-Bio Tech, ULiège, 5030 Gembloux, Belgium*
[b]*Quality and Authentication of Products Unit, Quality Department of Agricultural Products, Walloon Agricultural Research Centre (CRA-W), Chaussée de Namur 24, 5030 Gembloux, Belgium*
**Corresponding author*

Keywords:

Sucrose esters, HLB, Oleogels, Foam-template, Ethanol

Abstract

Sucrose esters (SE) have been widely studied as emulsifiers to tailor crystallization in fats. Nevertheless, few studies have assessed the potential of SEs as oleogelators to structure oleogels. This study aimed to evaluate alternative routes that would improve the oleogelation capacity of commercial SEs with different Hydrophilic-lipophilic balance (HLB) values and evaluate the physical properties of the oleogels produced by different routes. Four SEs were evaluated (SP10-HLB2, SP30-HLB6, SP50-HLB11, and SP70-HLB15) using three oleogelation routes (traditional or melting, ethanol, and foam-template). Of all evaluated samples, only the SP50 ethanol route with 10 % SE showed a solid-like structure. This sample presented the highest hardness (0.4 ± 0.1 N) and elastic modulus (4589 ± 89 Pa). SP70 showed a potential oleogel after foam-template approach due to the higher oil binding capacity. SP10 was the only directly completely soluble SE in oil, although it formed a very liquid gel. SP30 did not show a potential or oleogel structure for any of the routes tested.

1. Introduction

Sugar esters (SEs) have been known since the 1960 s. SEs are non-ionic surface-active agents derived from esterification (fatty acids and sucrose) or transesterification (fat and sucrose) reactions. SEs of fatty acids are emulsifiers, obtained by esterifying one or more hydroxyl groups of the sucrose molecule with edible fatty acids. The fatty acids react with one or more of the hydroxyl groups of sucrose to form mono-, di-, tri- or higher esters (**Fig. 1**A). They are tasteless, odorless, and non-toxic and have been explored as emulsifiers for foodstuffs or stabilizing agents in medications and cosmetics

Published in : Food Chemistry (2023), vol. 405, Part B, 134927
DOI: 10.1016/j.foodchem.2022.134927
Status : Postprint (Author's version)

because they are non-irritant to the eyes and skin (Angéla Szuts et al., 2007; Angela Szuts & Szabó-Révész, 2012).

The most common fatty acids used in SEs are lauric (La), myristic (M), palmitic (P), stearic (St), oleic (O), behenic (Be), and erucic (E) acids (Szuts & Szabó-Révész, 2012). They can exist as solids, waxy materials, or liquids. A wide variety of SEs can be obtained by changing the nature or number of the fatty acid groups, producing products with a varied range of HLB, from 1 to 16 (Angela Szuts & Szabó-Révész, 2012; Ye & Hayes, 2014). The HLB value is associated with mono-, di- and higher esters formed and their solubility in water. The solubility of the monoesters in water is good, and they usually form the majority of the high hydrophilic SEs (HLB 10–16). On the other hand, di- and higher esters are not water-soluble, and depending on their proportion in the SEs they can form medium HLB (7–9) that are water dispersible and low HLB (0–6) that are hydrophobic (oil soluble). Depending on the degree of esterification, SEs decrease the surface tension of water. They also exhibit different solubilizing abilities and foaming properties (Husband et al., 1998; Angela Szuts & Szabó-Révész, 2012; Ye & Hayes, 2014).

Subsequently, the final application of the SEs depends on their content of monoesters, HLB, and the size of the esterified fatty acid chain. They have been used in pharmaceutical, cosmetic and food industries as emulsifiers (HLB low to high), dissolution improvers (high HLB), sustained and controller releasers (HLB low to high), enhancements of absorption/penetration (high HLB with C12-14 fatty acids), and lubricants (low to medium HLB) (Angela Szuts & Szabó-Révész, 2012). In the food industry SEs are essentially used in sauces, dressings, mayonnaise, caramels, chocolates, marshmallow, and bakery products (Nelen et al., 2015).

A big challenge in using SEs is dispersing them in a non-polar medium, such as fat and oils. The challenge arises from the hydrophilic monomers of SEs, which tend to aggregate. An alternative is the use of high-temperature mixing. However, it is not a solution for all types of SEs, indeed the higher the HLB values the less dispersed they are in the lipid phase, even at higher temperatures (Chansanroj & Betz, 2010; Angela Szuts & Szabó-Révész, 2012). For this reason, most of the studies involving SE in the lipid phase as emulsifiers have been performed using very low HLB SEs (1 or 2), regardless of the fat matrix (Cheng et al., 2021; Domingues et al., 2018; Fontenele Domingues et al., 2015; Rincón-Cardona et al., 2014; Rodríguez-Negrette et al., 2021; Tangsanthatkun & Sonwai, 2019).

Recently, besides as emulsifiers, SEs have been explored in lipid systems as oleogelators to form oleogels (Lu et al., 2016; Sintang et al., 2017; Willett & Akoh, 2019). In the last decade, the interest in oleogels has risen from the necessity of "healthy fats" with no trans and low in saturated fatty acids. By definition, oleogels are liquid oils structured by the addition at low concentrations (≤10 % w/w) of compounds (oleogelators) to form a network and entrap liquid oils (Co & Marangoni, 2012). An ideal oleogelator used in food applications must be food-grade, economically viable, efficient, versatile, and match the final product's physical properties (Vieira et al., 2015).

Different SEs have been tested as oleogelators using a *traditional* route (melting at high temperature) for SEs dissolution. A previous study has found that SEs using this route have a low structuration power, and that at least 20 % (w/w) of SE is necessary to form a stable gel (Lu et al., 2016). In order to reduce the amount of SEs necessary to form good oleogels, binary blends have been explored with lecithin (Sintang et al., 2017) and ascorbyl palmitate (Willett & Akoh, 2019). These authors found out that the

Published in : Food Chemistry (2023), vol. 405, Part B, 134927
DOI: 10.1016/j.foodchem.2022.134927
Status : Postprint (Author's version)

total amount of oleogelator could be reduced to 10 or 12 %, with SE concentration as high as 7 % in a blend if synergic combinations were formed (Sintang et al., 2017; Willett & Akoh, 2019).

Besides the *traditional* route, due to the foamability of the SEs (Husband et al., 1998), oleofoams using SE have also been explored. Oleofoams are another alternative to "healthy fats", they are colloidal dispersions of gas in a continuous liquid oil phase (Liu & Binks, 2021). When compared to the *traditional* route, the stability of the foam over time was improved when SEs were combined with other oleogelators such as lecithin (Patel, 2017). Moreover only 10 % of lipophilic SE seemed already enough to form a good oleofoam (Patel, 2017).

Different gel approaches involved water in the system to form hydrogels with high HLB SEs (Angéla Szuts et al., 2010), bigels (Golodnizky & Davidovich-Pinhas, 2020), or emulsions (Garti et al., 1999; Watanabe et al., 2018). Based on the potential of SEs for food and non-food applications and improvement of the oleogel properties based on different oleogelation routes developed in recent years, the objective of this study is to evaluate alternative routes that would improve the oleogelation capacity of different commercial SEs with different HLB values and evaluate the physical properties of the oleogels produced by different routes, and this using a maximum of 10 % SEs.

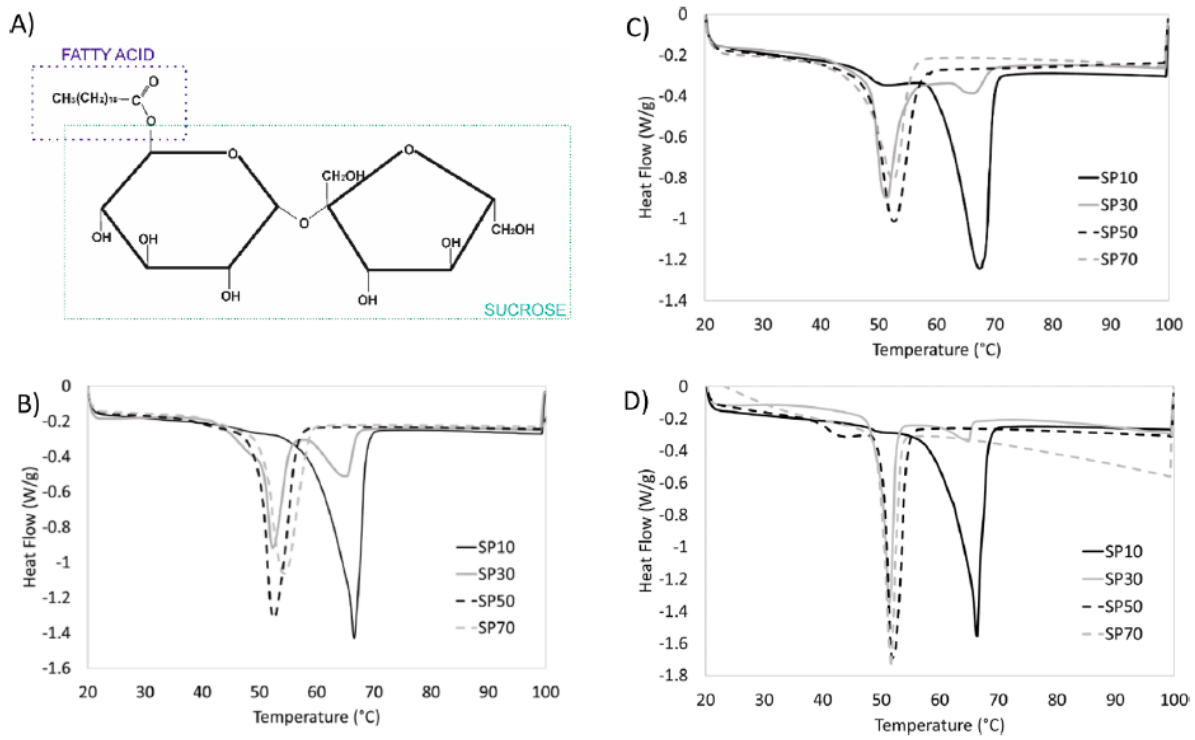

Fig. 1. The chemical structure of a sucrose esters (A). Melting curves for the sucrose esters powder traditional (B), treated with ethanol (C) and foam template (D).

Published in : Food Chemistry (2023), vol. 405, Part B, 134927
DOI: 10.1016/j.foodchem.2022.134927
Status : Postprint (Author's version)

2. Material and methods

2.1. MATERIALS

Four commercial SEs samples (all stearate/palmitate) were kindly donated by Sisterna (The Netherlands). SP10 is a stearate/palmitate oligo ester, HLB 2 with 10 % monoester. SP30 is a stearate/palmitate sucrose ester, HLB 6 with 30 % monoester. SP50 is a stearate/palmitate sucrose ester, HLB 11 with 50 % monoester. SP70 is also a stearate/ palmitate ester, HLB 15, and 70 % monoester. Rapeseed oil (RO) was acquired from Royale Lacroix (Flemalle, Belgium). RO was mainly composed of unsaturated triacylglycerols: triolein (OOO, 29.3 %), dioleoyl-linoleoyl glycerol (OOL, 22.6 %), dioleoyl-linolenoy (OOLn, 12.1 %), and dioleoyl-palmitate glycerol (POO, 6.5 %).

2.2. OLEOGEL PREPARATION

The four different SEs (SP10, SP30, SP50, and SP70) were used to prepare oleogels using three different structuration routes: (1) TRADITIONAL (without any pre-treatment, using only high temperature [90 °C] dissolution), (2) ETHANOL (sample pre-dissolved in ethanol), and (3) FOAM (using a foam-template pre-treatment). 50 mL of oleogel was prepared in triplicate for each route, and the total amount of SE used was always fixed at 10 % (w/w) in rapeseed oil.

The *traditional route* oleogels were prepared by melting the SE in pre- heated rapeseed oil (90 °C) under 350 rpm magnetic stirring for 20 min. After complete dissolution of the material, the oleogel samples were cooled statically to 20 ± 0.05 °C at approximately 0.5 °C/min, and stored for 48 h at 20 °C in an incubator for network stabilization.

The ethanol method was based on a first dilution of the SE powder in ethanol 97 % (5 g of SE for 20 mL of ethanol). The blend ethanol + SE was further mixed in pre-warmed rapeseed oil (45 mL, 90 °C). Samples were then kept at 90 °C for one hour for ethanol evaporation, and then cooled to 20 °C and stored as described for the *traditional* method.

The foam template method was based on Patel et al. (2013). The SEs were first dissolved in 500 mL water (2 w/w), using a magnetic stirrer (500 rpm) for 5 h at 20 ± 2 °C. After the dissolution, the aqueous blend was stirred with an Ultraturrax (IKA, Werke, Germany) at 11000 rpm for 5 min and further frozen in an aluminum dish overnight at −50 °C. The frozen mixture was then freeze-dried for 72 h at −80 °C. The powder obtained was used to produce oleogels by adding the *foam*-template powder into the oil at room temperature (20 ± 0.05 °C). The blends were mixed using a magnetic stirrer (100 rpm) and stored in a 20 °C incubator for 48 h, as for the two other routes.

2.3. METHODS

2.3.1. MICROSCOPY

The microstructure using polarized and non-polarized light was analyzed on an optical microscope (Nikon Eclipse E400, Kanagawa, Japan) equipped with a digital camera (Nikon, DS-Fi2, Tokyo, Japan).

Published in : Food Chemistry (2023), vol. 405, Part B, 134927
DOI: 10.1016/j.foodchem.2022.134927
Status : Postprint (Author's version)

One drop of the stabilized sample was placed between a slide and a cover slide, and analyzed immediately. For each sample, eight images of the three different replications were analyzed. The images were analyzed using an image processing software (NIS-D, v 4.2, Nikon, Tokyo, Japan).

2.3.2. OIL LOSS

The amount of oil loss of the samples was evaluated by centrifugation, using a 5810R Eppendorf centrifuge (Hamburg, Germany), according to da Silva and Danthine (2021). First, a pre-weighed empty 2 mL Eppendorf (wa) was filled with approximately 1 g of sample. The systems sample + Eppendorf were also weighted (wb) and centrifuged for 15 min at 2950 *g* at 20 °C. Subsequently, the tubes were left upside down to drain the free oil for 10 min. The drained Eppendorf's were weighted once more (wc). The test was performed in quadruplicate and the oil loss was calculated according to **Eq. (1)**:

$$Oil\ loss\ (\%) = [(wb - wc)/(wb - wa) * 100] \quad (1)$$

2.3.3. RHEOLOGY

Rheology experiments were performed at 20 °C using a Modular Compact Rheometer MCR 302 (Rheoplus, Anton Paar, Austria). The Rheoplus software (Anton Paar, Austria) was used to analyze the rheological parameters. A plate-plate geometry with a diameter of 40 mm was used and the gap was set to 1000 µm. Strain sweeps were conducted from 0.0008 to 100 % strain at 1 Hz. The linear viscoelastic region (LVR) was calculated as the strain value where G' was constant. Frequency sweeps (0 to 100 Hz) were also measured with an amplitude fixed at 0.01 %. These analyzes were performed in quadruplicate.

2.3.4. TEXTURE

A Texture Analyzer (TAXT plus, Stable Micro Systems, UK) equipped with a 5 kg load cell was used to determine the mechanical properties of the oleogels. A penetration analysis test was performed using a 5-mm diameter cylinder probe. The probe penetrated 1 mm/s for 10 mm. The hardness was expressed as the maximum force of the peak (N). Analysis was performed in triplicate.

2.3.5. MELTING PROPERTIES

The melting curves were obtained using a Q2000 DSC (TA Instruments, New Castle, DE, USA) coupled with a refrigeration cooling system (TA Instruments, New Castle, DE, USA) and calibrated with indium and eicosane. About 5–8 mg of oleogel and oleogelators were weighed in a Tzero hermetic pan and heated from 20 °C to 100 °C with 5 °C/min as heating rate. A similar Tzero hermetic empty pan was used as a reference, and the melting curves were analyzed using the Universal Analysis Software version 4.2 (TA Instruments, New Castle, DE, USA). The parameters evaluated were onset temperature (T_{on}), peak temperature (T_p), and enthalpy (ΔH). The analysis was performed in triplicate.

The melting point of the SEs was also measured by DSC using a Tzero hermetically sealed pan. In this case, the samples were first heated to 100 °C using a 5 °C/min heating rate and kept at 100 °C for 30 min to ensure complete melting; after this, they were crystallized using a 5 °C/ min cooling rate until −20 °C and kept at this temperature for 90 min. The last step was a second melting to 100 °C, at a 5

Published in : Food Chemistry (2023), vol. 405, Part B, 134927
DOI: 10.1016/j.foodchem.2022.134927
Status : Postprint (Author's version)

°C/min heating rate. The peak temperature (T_p) obtained from the last melting step was used to quantify the melting point (Kerr et al., 2011).

2.3.6. X-RAY DIFFRACTION

The X-ray diffraction (XRD) measurements were performed at 20 °C using a Bruker D8 Advance Diffractometer (Bruker, Germany) in both the long and short spacing regions (2θ from 1 to 27°), using a 0.02° as step size with 135.01 s by step. The instrument was equipped with a LynxEye detector (Bruker, Germany) and with a Cu Kα radiation (λ = 1.54178 Å, 40 kV, 30 mA). Data was analysed with the Diffrac.Eva software (Bruker, Germany).

2.3.7. MIR ANALYSIS

The ATR-FT-MIR spectra of oleogels were acquired using a Bruker Vertex 70 Fourier transform spectrometer equipped with an ATR golden gate accessory. The spectra were acquired (4000–600 cm^{-1}) with a resolution of 4 cm^{-1} with 64 co-added scans. The spectral acquisition was done using OPUS 6.5 (Bruker) software. The reference spectrum used was the air spectrum collected before each sample analysis. The analysis was done in triplicate.

2.3.8. STATISTICAL ANALYSIS

Each process and analytical measurement was performed in replicates as described above. Data shown are mean values and standard deviations of the mean. Statistical differences amongst treatments were assessed using 2-way ANOVA ($\alpha < 0.05$), and correlation analyses were performed using GraphPad Prism version 8.0 (La Jolla, CA).

3. Results and discussion

3.1. OLEOGELATOR CHARACTERIZATION

3.1.1. MELTING POINT

The SEs powders naturally had different melting curves and melting points, as shown in **Fig. 1.** The SP10 showed a higher melting point (66.5 ± 0.1 °C) and melting enthalpy (85.2 ± 1.3 J/g), in agreement with data reported by Tangsanthatkun and Sonwai (2019) for similar HLB SE (S-170, HLB 1) which showed similar T_p ~ 65 °C. Among the four SE considered in our study, SP30 was the only one that showed two melting peaks: one at a 52.0 ± 0.2 °C and the other at 65.0 ± 0.1 °C. In SP30 case, the total melting enthalpy was 64.9 ± 0.4 J/g, where around 20 J/g (about 30 %) were from the higher melting peak. This can be correlated with the increase in the concentration of monoesters (30 %) in the SP30 ($p = 0.02$, $r = -0.80$). It was previously reported that lipophilic SEs with intermediate HLB (3–5) as C-1805 (HLB 5) and S370 (HLB 3) also showed two endothermic peaks at 48.5 °C and 63.6 °C for the C-1805 (Liu & Binks, 2021), and at 54 °C and 64 °C for the S370 (Chansanroj & Betz, 2010; Angéla Szuts et al., 2007). SP50 and SP70 *traditional* powders showed only one endothermic peak, close to the SP30 lower melting peak (SP50: 52.4 ± 0.1 °C; 61.7 ± 0.4 J/g and SP70: 54.1 ± 0.7 °C; 61.7 ± 0.4 J/g). Similar

Published in : Food Chemistry (2023), vol. 405, Part B, 134927
DOI: 10.1016/j.foodchem.2022.134927
Status : Postprint (Author's version)

high HLB SE melting points and melting profiles formed by only one peak have been observed previously (Chansanroj & Betz, 2010). The transition to only one peak confirms the monoester's influence in the melting profile. Likewise, Angéla Szuts et al. (2007) revealed that the melting points and melting ranges of SEs with lower HLB values were higher and sometimes with more peaks, probably because SEs with high HLB values usually included only mono-, di- and tri-esters, while the SEs with lower HLB values contained tetra- and pentaesters too.

Using alternative routes for the SP10 (**Fig. 1**B and C) did not cause any expressive changes in the melting profile of the prominent melting peak. The sample kept the same melting point (66.5 °C) and a very high melting enthalpy ~ 85 J/g. The sole change that was observed was a shoulder formed at a lower T_p (50.9 ± 1.1 °C) for either *ethanol* or *foam* treatment. This suggests that in these samples the treatments somehow increased the monoester's potential to connect even in low SEs concentrations (10 % w/w) or that the treatments had separated the monoester from the other major constituents of this SE, resulting in more noticeable effect after the *ethanol* treatment. In the SP30, a reduction in the peak at higher temperature (65.0 °C) and an increase in the lower melting point peak (52.2 °C) after *ethanol* treatment were observed, this was even more pronounced after *foam*-templated treatment. SP50 and SP70 did not form an additional peak after the treatments; no peak reduction, or changes in T_p were observed. Compared to their corresponding *traditional* powders, a reduction in enthalpy using *ethanol* and *foam*-template treatments was observed. That reduction was more pronounced for SP70 (around 20 J/g smaller) than for SP50 (only about 10 J/g). No shoulder or additional melting peak could be observed on these two samples.

3.1.2. POLYMORPHISM

The X-ray diffraction patterns of the SE powders can be seen in **Fig. 2.** It is reported by Jandacek and Webb (1978) that sucrose polyester packs similar to α and β' phase of TAGs. All SEs, regardless of the pre-treatment in the wide-angle (15–27°), showed only one diffraction peak at around 4.15 Å, suggesting the α polymorphic form. SEs of La, M, P, St, and E acids, which solidified from the melt, typically have diffraction patterns identical to those of the α-phase of analogous triglycerides (Jandacek & Webb, 1978).

In the small angles region (1–15°), SP10 presented a main peak corresponding to a distance of 53.4 Å (001), followed by its higher order reflection peaks observed at 2θ, 002 and 003 (**Fig. 2**). Similar distances were found for more complex SEs structure formed by polyesters (S970) (Angéla Szuts et al., 2007). Patterns that indicate a double chain length structure and a hexagonal lateral packing (Rincón-Cardona et al., 2014).

SP50 and SP70, on the other hand, regardless of the treatment performed, did not show this signal of a 2L packing at about 53 Å. They nevertheless showed a main peak (around 36 Å) with a higher order reflections at 18 Å, peaks that suggest a 001 of 72 Å. These reflections have been reported as 3L packing for fats (Lopez et al., 2005), or spherical micelles for previous studies in SE (Garti et al., 1999; Husband et al., 1998; Kawaguchi et al., 1991; Sintang et al., 2017). SP30 has an intermediate behavior (as observed in the DSC melting curves) since it shows both patterns (54 Å and 72 Å). It could be assumed that the change in the X-ray pattern could be related to the content of monoesters, which is in agreement with a previous study (Husband et al., 1998).

Published in : Food Chemistry (2023), vol. 405, Part B, 134927
DOI: 10.1016/j.foodchem.2022.134927
Status : Postprint (Author's version)

3.1.3. MIR ANALYSIS

Fig. 2 (second column), shows the mid-infrared spectra of the SEs. The main absorbance bands for the SEs are shown in SP10 **Fig. 2**, and has been described previously in the literature. It can be attributed as O–H stretch of free hydroxyl in sucrose (3420–3500 cm^{-1}), the ester C=O between 1740 and 1750 cm^{-1}; and the glycosidic bond stretch for sucrose between 1728 and 995 cm^{-1} (Kondamudi & McDougal, 2019; Liu & Binks, 2021; Youan et al., 2003).

In general, regardless of the pre-treatment, all samples showed similar spectra with absorbance bands centred around the same frequencies, which would be expected since they all showed similar chemical bonds. The most observed difference can be attributed to the absorbance intensity variations of these bands. The band of the O–H stretch had a lower absorbance intensity for sample SP10 (all treatments) compared to the other higher HLB samples, and in general, this band was even more pronounced after *ethanol* and *foam* treatments.

These suggest that more O–H groups are present in the sample due to the higher HLB in samples SPs 30, 50, and 70 and the pre-treatment.

The increase in HLB was followed by an increase in the intensity of the glycosidic bond stretch for sucrose (900–1050 cm^{-1}). This result was previously observed and attributed to the increased hydrophilicity and hydrogen bonding capability of the SE of higher HLB (Youan et al., 2003). Interestingly, for SP30, the *traditional* sample due to the low HLB showed a shallow band between 900 and 1050 cm^{-1}, compared to the samples treated with *ethanol* or *foam*-template, which confirms that the treatments strongly influenced this sample. In addition, the higher absorbance intensities of the – CH_3 and – CH_2 stretching's, which occur from 2975 to 2950 cm^{-1} and from 2885 to 2865 cm^{-1} in sample SP10 *traditional*, confirm the highest hydrophobic moieties in this sample (Youan et al., 2003).

Published in : Food Chemistry (2023), vol. 405, Part B, 134927
DOI: 10.1016/j.foodchem.2022.134927
Status : Postprint (Author's version)

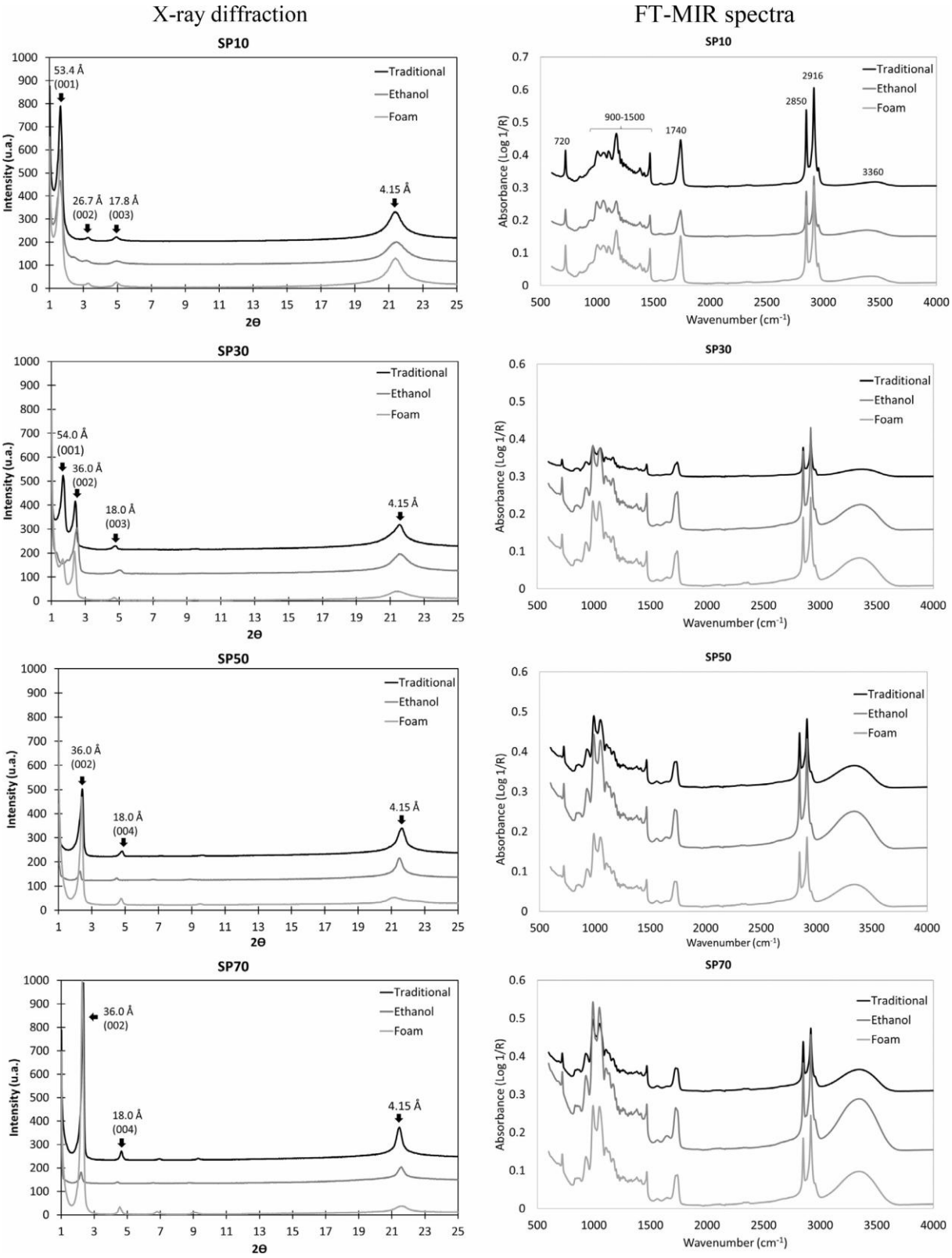

Fig. 2. X-ray diffraction (column 1) and FT-MIR spectra (column 2) of the sucrose esters oleogelators using different previous treatments. Values indicated in Å in column 1 corresponds to d/n.

Published in : Food Chemistry (2023), vol. 405, Part B, 134927
DOI: 10.1016/j.foodchem.2022.134927
Status : Postprint (Author's version)

3.2. PHYSICAL PROPERTIES OF THE OLEOGELS USING DIFFERENT OLEOGELATION ROUTES

3.2.1. MICRO AND MACROSTRUCTURE

The macroscopic and microscopic structure of the SEs oleogels using the different oleogelations routes can be observed in **Fig. 3**. As expected, due to the high HLB value, samples SP50 and SP70 were not soluble in oil and formed several lumps; only samples SP10 and SP30 dissolved using the *traditional* high-temperature route. The SP10 dissolution was even better than SP30 since some lumps were still observed in the SP30 using the *traditional* route (**Fig. 3**). Even at high temperatures (90 °C; higher than their melting point), hydrophilic SEs did not completely "melt". They only turn into a glassy state (Angéla Szuts et al., 2007). Consequently, the hydrophilic SEs aggregated together even at high temperatures due to solid attractions by their polar head, which explains the lumps observed within these samples (Chansanroj & Betz, 2010). Nevertheless, even the oil-soluble SEs did not form a solid-like oleogel using the *traditional* route; a similar weak structuration for a SE similar to SP10 was observed previously in a sunflower oleogel using the *traditional* route (Sintang et al., 2017). Liu & Binks reported that a SE with HLB 5 formed a turbid viscous dispersion at 25 °C within the two-phase region where surfactant crystals coexist with an oil solution of surfactant at its solubility (Liu & Binks, 2021). These results are also in agreement with Lu and others (2016), since they have reported that at least 20 % of SE with low or medium HLB (1 and 9) are necessary to form stable gels.

Observing the "gels" microstructure, SP10 formed a very homogeneous and compact structure, made of several tiny polydispersed globular crystals, as previously formed using sucrose palmitate and stearate in fat blends (Garbolino et al., 2005), in sunflower oil (Sintang et al., 2017), and in olive oil (Liu & Binks, 2021). The size and shape of the crystals did not change very much in samples SP30, SP50, and SP70 using the traditional route. Still, fewer and fewer crystals were observed in higher HLB samples due to the decrease in oil solubility. HLB values have previously been correlated to a fast crystallization rate. Subsequently, SE with a HLB value of 2 is a likely contributing factor to the growth of numerous small crystals (Willett & Akoh, 2019). Although more crystals were formed, the type of crystal directly influenced the oil entrapment, in this case the formation of polydispersed globular crystals explained the very low structuration power of the SE in oil, because although high in density, this type of crystal does not form a well- connected crystal network (Sintang et al., 2017).

Some visual and microstructural changes could be observed using the *ethanol* route (**Fig. 3**). SP50, in this case, showed a better visual structuration, forming a solid-like structure. SP10 showed liquid gel, and SP30 and SP70 showed liquid gel with lumps. The more visually structured oleogel SP50 *ethanol* also showed the most organized crystalline network, where all crystals were interconnected and entrapped the liquid phase well. Two types of crystal forms were responsible for structuring SP50 *ethanol*: needles and globular morphology. The formation of needles was commonly observed before for palmitate/stearate sucrose esters (Garbolino et al., 2005). Samples SP30 and SP70 *ethanol* did not show any needles, only the polydisperse globular crystals. In both cases, a maltese cross was observed in some globular crystals (zoom in SP70 *ethanol*, **Fig. 3**). Large-size birefringent (maltese cross) crystals pierced out interfacial layers in a SE similar to SP70 (SP1570, HLB 15, 70 % monoester) (Zeng et al., 2021). In this previous study, the maltese cross crystals were formed at the air/oil interface for

Published in : Food Chemistry (2023), vol. 405, Part B, 134927
DOI: 10.1016/j.foodchem.2022.134927
Status : Postprint (Author's version)

oleofoams, where the product was also submitted to high agitation at a high temperature. SP10 *ethanol* showed a similar microstructure as the traditional route, but fewer crystals were observed in this case, suggesting that a weaker crystalline network was formed. Although no significant changes were observed in sample SP50, melting point, X-ray, and infrared for the *ethanol* treatment showed that, as for other samples, the crystalline network formed in oil changed expressively. This suggests that the proportion of 50 % of monoester (high hydrophilic portion) dissolute was improved by the *ethanol* route. This lead to a higher solubility of the SP50 in oil after the treatment and consequently a well-structured-oleogel was obtained.

After using the *foam*-template route, the more visually structured sample was SP70, followed by SP50. In contrast, SP30 and SP10 were very liquid. SP70 showed two structures in the network, one formed by small crystalline needles in the background and a non-crystalline structure on the top. The formation of a non-crystalline structure was only observed for SP70, even though all samples went through the same pre-treatment. This non-crystalline structure might be the SE's hydrophilic portion that opens up for oil bounding after the *foam*-template approach. Husband and coworkers demonstrated that a 4:1 M ratio of sucrose mono- and di-esters could display superior foaming properties due to interactions between these constituents (Husband et al., 1998). Soultani et al. (2003) observed that the foam height dropped with the increase of the fatty acid carbon number and the presence of diesters in the preparation. The fatty acids chain size was the same for all SE as they were all stearate/palmitate, which confirms that the better foamability of SP70 was due to the higher monoester content (70 %). The water high surface tension makes it difficult to disperse and retain air in a product. Adding SEs can reduce the surface tension, as they act as surfactant due to their amphiphilic properties (the polar sucrose moiety serves as hydrophilic part and the fatty acid chains serves as lipophilic part). Low HLB SEs act as water-in-oil emulsifiers while high HLB SEs act as oil-in-water emulsifiers, and emulsifiers with a high HLB value are the most effective at the formation and stabilization of foams, enabling incorporation and retention of air in a product. According to Nelen et al (2015), high HLB (11–16) sucrose esters are able to lower the surface and interfacial tensions and produce stable foams.

SP50 formed very long fibrous crystals, which were interconnected, explaining the viscous material formed. SP30 formed a microstructure similar to SP50, but less crystals were formed, and empty molecular spaces could be observed, confirming that the effectiveness of the foam- template route is more related to the hydrophilic part of the SEs (monoesters). SP10 again showed very small crystals agglomerated in circular clusters which were moreover not interconnected.

Published in : Food Chemistry (2023), vol. 405, Part B, 134927
DOI: 10.1016/j.foodchem.2022.134927
Status : Postprint (Author's version)

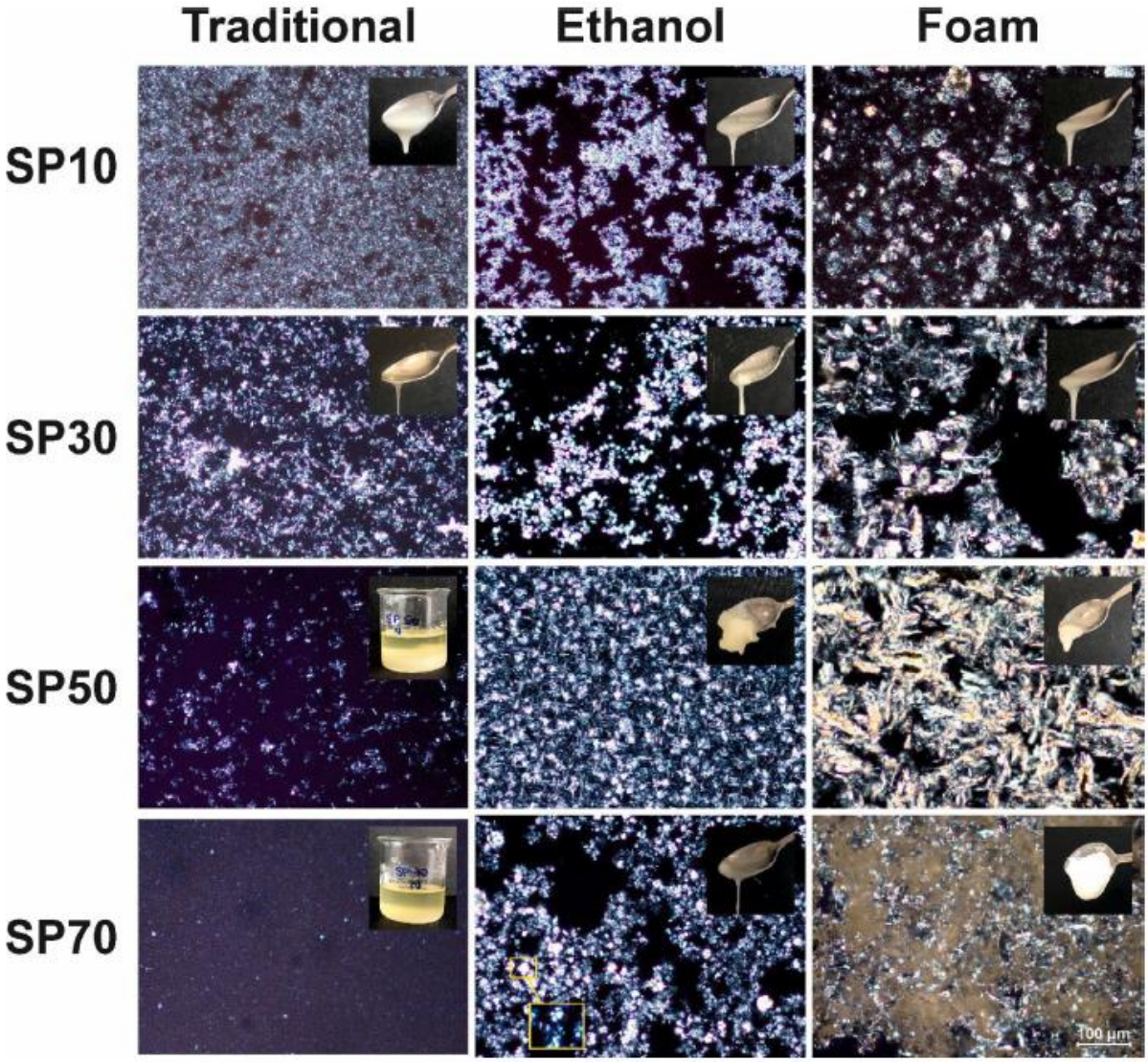

Fig. 3. Visual and microstructure images of the different sucrose esters oleogels using different structuration routes. Magnification 20x.

3.2.2. OIL LOSS

The network formed by the different routes and sucrose esters resulted in different oil loss, as shown in **Fig. 4**A. Samples with higher oil loss were SP50 and SP70 using the *traditional* route (95.6 ± 0.5 % and 95.34 ± 1.1 %, respectively), which was expected since those compounds were not soluble in oil and consequently could not form a network or entrap the oil. Nevertheless, these SEs showed a better oil entrapment when the alternative structuration routes were used. For SP50, both routes (*ethanol* and *foam*) showed a similar significant increase in the oil binding capacity compared to the *traditional* route ($p < 0.05$). The reduction in the oil loss was more than 50 %, which emphasizes the improvement in the bounds between the oil and the oleogelator using the *ethanol* or *foam* route. The SP70 oil loss showed a minor but significant improvement after *ethanol* treatment (79.0 ± 1.5 %, $p < 0.05$) and a highly expressed improvement after the *foam*-template approach (31.6 ± 1.2 %, $p < 0.05$). The SP70

Published in : Food Chemistry (2023), vol. 405, Part B, 134927
DOI: 10.1016/j.foodchem.2022.134927
Status : Postprint (Author's version)

foam had the lowest oil loss amongst all samples and structuration routes used. In SE oleofoams, the oil drainage occurs immediately after preparation leading to a dry foam within the first few hours, then foams gradually decay entirely via coarsening/coalescence (Liu & Binks, 2021). In our case, the SP70 *foam* was stored for 48 h, and centrifugation forced the oil leakage, indicating that the *foam*-template might be more promising to form stable oleogels with high HLB SEs. In other materials such as xhantana gum, gelatin, and hydroxypropyl methylcellulose, an oil binding capacity higher than 92 % was obtained using a similar *foam*-template approach (Abdollahi et al., 2020; Patel & Dewettinck, 2015), which confirms the potential of the route to improve oil loss.

SP30 showed a similar profile to SP70, where the highest oil loss was observed using the *traditional* route (83.2 ± 4.8 %), followed by the *ethanol* route (66.6 ± 2.1 %), and the lowest oil loss was observed after the *foam*-template approach (44.1 ± 2.4 %). Although the profile was similar, there was a difference in the magnitude of the results. SP30 showed significantly lower values than SP70 using the *traditional* and *ethanol* routes, but a significantly higher oil loss after the *foam* treatment ($p < 0.05$). The SP30 and SP70 profile similarity was not expected since they both had very different HLB values. However, with a medium–low HLB, with only 30 % of monoesters, SP30 behaves like a high hydrophilic SE. SP10 was the only sample where the *traditional* route showed the lowest oil loss (54.8 ± 2.1 %). In this case, any additional treatment to the SE reduced the oil binding capacity of the oleogelator.

A high ability to entrap oil by needle-like crystals in oleogels was previously reported by other groups (Blake et al., 2014; Blake & Marangoni, 2015; Doan et al., 2015; Fayaz et al., 2020). This is because a needle-like structured network has a higher crystal surface area, compared to other crystals such as discs and spherulites, that improves oil entrapment. These hypotheses can be correlated with the microstructure results observed in **Fig. 3**. A higher oil binding capacity for each SE was found when samples were structured by needles which formed a more organized network able to entrap more oil such as SP10 *traditional*, SP50 *ethanol* and *foam* and SP70 *foam*.

Although the different structuration routes significantly changed the oil binding capacity of the SEs, the amount of oil loss was still very high (at least 30 %) using 10 % of oleogelator. The result follows the previously discussed deficient structuration power of SE, where at least 20 % would be needed to form a solid-like structure (Liu & Binks, 2021). However, the benefits of these new routes could be combined with other oleogelators to form binary or ternary systems with an improved oil binding capacity, as previously shown for the combination of SE: lecithin, which would make SE a feasible oleogelator for food applications (Sintang et al., 2017).

Published in : Food Chemistry (2023), vol. 405, Part B, 134927
DOI: 10.1016/j.foodchem.2022.134927
Status : Postprint (Author's version)

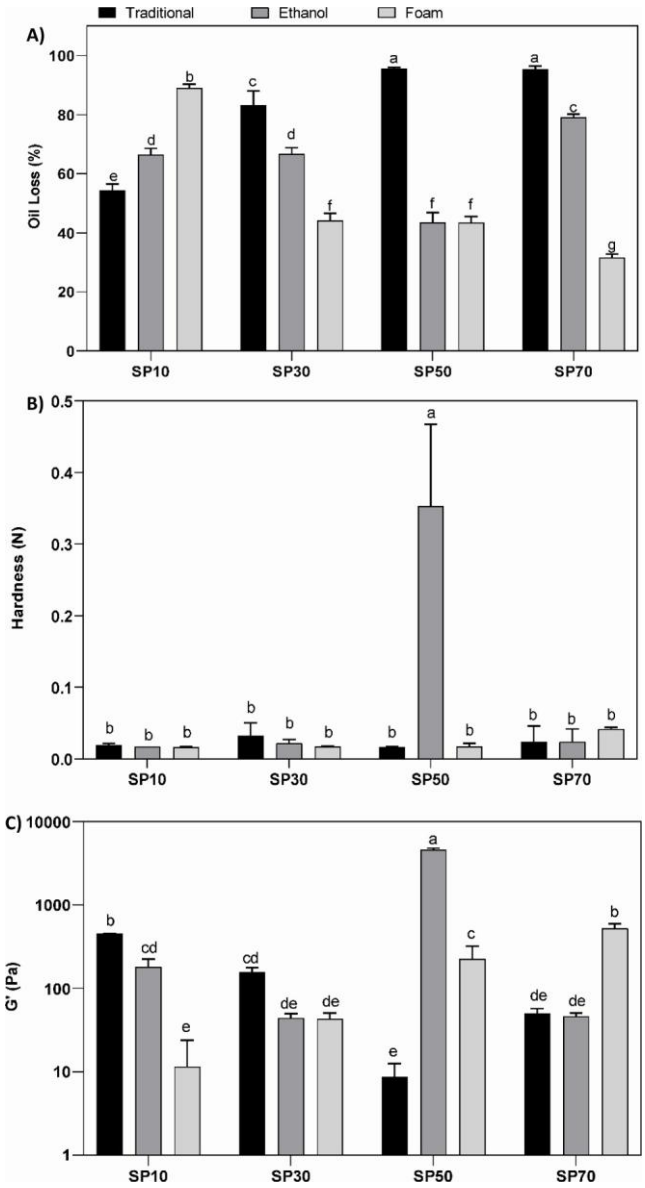

Fig. 4. Oil Loss (A, %), hardness (B, N), and elasticity (C, G'-Pa) of the sucrose esters oleogels structured using different routes.

3.2.3. MECHANICAL PROPERTIES

The mechanical properties of the oleogels are shown in Fig. 4. All oleogels except SP50 ethanol showed extremely low hardness (Fig. 4B), with no differences between them ($p > 0.05$). Compared with the visual observations, this result was expected since this sample had a more "solid-like" visual structure. Although SP70 foam also formed a visual semi-solid structure, with a well-connected network (Fig. 3) that resulted in a better oil binding capacity, the hardness of this sample was similar to the other liquid samples. SEs with P or St fatty acids that formed a network structured by small crystals showed a potential to increase the hardness in palm blends. In contrast, samples with low hardness showed the presence of large crystals and a very inhomogeneous microstructure. This indicates that the size of the crystals and, in particular, the interactions among the crystals led to the formation of a fat crystal

Published in : Food Chemistry (2023), vol. 405, Part B, 134927
DOI: 10.1016/j.foodchem.2022.134927
Status : Postprint (Author's version)

network, which was primarily responsible for the macroscopic textural properties of the samples (Garbolino et al., 2005).

Observing the elasticity (**Fig. 4**C), more significant differences were observed among the samples in the linear viscoelasticity region.

Nevertheless, the results were similar to the hardness ones, and SP50 *ethanol* also showed the highest value for elasticity (4589 ± 89 Pa), confirming that this sample had a more rigid and more elastic behavior compared to the other SEs or others routes ($p < 0.05$). This result can also be attributed to the crystalline network formed after the *ethanol* route and affirms the positive correlation between hardness, viscoelasticity, and microstructure ($p < 0.01$ $r = 0.99$).

The second highest elasticity was found for SP70 *foam* and SP10 traditional, and they were similar to each other ($p > 0.05$). Observing the microstructure of these two samples, they also showed a high density of tiny crystals in a highly organized network.

SP50 *foam*, SP10 *ethanol*, and SP30 *traditional* showed the third-highest elasticity values. Nevertheless, SP30 *traditional* was not statistically different from other routes using the same SE. This suggested that SP30 does not have a best route among all routes tested, and they all formed similar very soft oleogels. In emulsions, the rheological behavior of SEs was previously evaluated and was found to be influenced by the SE concentration, the presence of lipid co-surfactants or oil, and the mode of preparation (Rodriguez-Abreu et al., 2005). In this study, we used different SE and routes, which seemed to affect the SE oleogels significantly. For drug delivery, the presence of more significant amounts of monoesters in the SE with increasing hydrophilicity resulted in enhanced elasticity and tensile strength (Chansanroj & Betz, 2010), what seems to be true for the oleogels if the solubility in oil is solved by using alternative routes.

3.2.4. POLYMORPHISM

In **Fig. 5**, the X-ray profiles of the SE oleogels can be observed. Similar to what was observed in the powders, 4.15 Å was the only diffraction peak in the wide-angle region for all samples, regardless of the structuration route used. Different SEs have shown similar results with different HLB contents in different fat sources (Domingues et al., 2018; Liu & Binks, 2021; Sintang et al., 2017; Angéla Szuts et al., 2007). The significant difference observed in the wide-angle from **Fig. 2** to **Fig. 5** is that the peak is less visible and is at the top of a significant liquid phase, generally found in high oil content samples such as oleogels. This suggests that the mixture of the SE in oil has not changed the SE's polymorphic form and it remained in the α-form.

In the small angle region, sample SP10 and SP30 showed a similar profile as the powder. SP10 in all treatments and SP30 traditional presented a distance at 53.4 Å (001 peak). SP30 ethanol showed a predominance of the 002 reflection at 36 Å (possible 72 Å as 001) and SP30 foam a combination of both.

On the other hand, high HLB samples SP50 and SP70 showed a prominent reflection order at 38 Å, however using the foam template approach this reflection dislocated to a lower 2θ. This could be attribute to a reverse configuration of the micelle due to the polarity of the solvent, as previously observed by Rodriguez-Abreu et al. (2005).

Published in : Food Chemistry (2023), vol. 405, Part B, 134927
DOI: 10.1016/j.foodchem.2022.134927
Status : Postprint (Author's version)

3.2.5. MELTING BEHAVIOR

The melting curves for the SEs oleogels using the different structuration routes can be observed in **Fig. 5** (right column). SP10 oleogels showed a similar profile using *traditional* and *ethanol* route, characterized by a single narrow melting peak in a high melting temperature (T_p, 65.0 ± 0.5 °C) with a similar melting enthalpy (ΔH 7.3 ± 1.2 W/g). This high T_p was expected due to the highest melting point found for SP10 (66.5 ± 0.1 °C) and in agreement with a previous research using 10 % of SP10 in sunflower oil (Sintang et al., 2017). The low HLB SE oleogels have higher melting temperatures due to the higher melting point of the St and P acids present and their higher interaction and solubility in non-polar oils (Willett & Akoh, 2019). The *foam*-template approach in the SP10 changed the melting profile to a broader peak with the addition of a visible shoulder around 50 °C, followed by a significant reduction in T_p of the prominent melting peak to 63.0 ± 0.1 °C, and an increase in the ΔH (10.3 ± 2.4 W/g). This route might have increased the intermolecular hydrogen bonding of the SP10 with the oil, which influences the shape of the melting behavior of oleogels (Sintang et al., 2017).

SP30 also showed similar peaks using *ethanol* and *traditional* routes with T_p around 49 °C for both routes and ΔH around 4 W/g. Values are a lot lower than SP10, which can be attributed to the higher amount of hydrophilic portion that was not soluble in the oil. The *foam*-template in SP30 also has a broader melting peak but at a higher temperature. Oleofoams of similar SE also formed a shoulder at a much higher temperature (~65 °C) in a similar SE (Liu & Binks, 2021).

SP50 was affected by all routes, and the *traditional* SP50 showed a similar melting profile to SP30 with a significantly similar T_p and ΔH ($P < 0.05$). SP50 *ethanol* showed a peak with the same enthalpy but dislocated to a lower temperature (46.3 ± 1.7 °C). Previously, oleogels that formed a more organized crystalline network, with more and smaller interconnected networks, showed a lower T_p during melting, suggesting a better co-crystallization between the oleogelator and the oil (Doan et al., 2015). On the other hand, after the *foam* route, the peak had a higher enthalpy with similar T_p as SP50 *traditional*, which suggested more material was melted after the *foam* treatment. This confirms our hypotheses that the *foam* improved the solubility of the SE, and consequently, more SE was bonded to the oil. This result is observed as well in **Fig. 3**.

SP70 oleogels showed a different profile, with the SP70 *traditional* showing two melting peaks (around 40 and 50 °C). This result suggested that two portions of the SP70 was forming two different structures. When SP70 were structured using other routes, a single peak was observed, one at a lower T_p for SP70 *ethanol* (45.0 ± 1.3 °C) and at a higher T_p for SP70 *foam* (51.0 ± 0.2 °C). The formation of a single peak indicates simultaneous crystallization of various compounds (co-existence), a mixed crystal, or both in the oleogelator (Tavernier et al., 2017). Although both treatments formed a unique melting peak, indicating a co-existence among the hydrophilic and hydrophobic portions, they showed significantly different T_p and enthalpies. This suggests that both routes improved the structuration of the high HLB SE in oil. Nevertheless, the *foam*-template for the SP70 is more efficient, as observed by the other physical properties previously analyzed.

The improved solubility of SE in oil in the *foam*-template could be explained by previous observations for cellulose derivatives where the *foam* stabilization property was attributed to the gelled film formation of the polymer at the air water interface (Patel et al., 2013); for SEs a similar behavior can be expected. First they are dissolved in water and air bubbles are induced by high mixing, the high

Published in : Food Chemistry (2023), vol. 405, Part B, 134927
DOI: 10.1016/j.foodchem.2022.134927
Status : Postprint (Author's version)

concentration of monoester in SP70 favored this dissolution and the formation of air bubbles. These air bubbles were more stable with a high amount of monoester because of the higher surface tension of the monoester compared with others di, tri and polyesters. After freeze-drying, the porous material formed showed an excellent oil absorption property with a high swelling capacity.

The melting data, T_p and enthalpy, were correlated to each other ($p = 0.01$, $r = 0.68$). Moreover, the monoester content was correlated with T_p ($p < 0.01$, $r = -0.81$). These results confirmed that a higher amount of monoesters showed a lower T_p, especially after the alternative routes, and lower T_p also resulted in lower enthalpy.

3.2.6. MIR ANALYSIS

The MIR spectra for the oleogels and rapeseed oil can be seen in **Fig. 6**. The major peaks that represent triglyceride functional groups in oils and fats are observed around 2937 cm^{-1} (C–H stretching (asymmetry)), 2856 cm^{-1} (C–H stretching (symmetry)), 1749 cm^{-1} (C=O stretching), 1454 cm^{-1} (C–H bending (scissoring)), 1166 cm^{-1} (C–O stretching and C–H bending), and 709 cm^{-1} (C–H bending (rocking)) (Guillen & Cabo, 1997). These bands were all observed in the rapeseed oil (**Fig. 6**). The main differences observed between **Figs. 2** and **6** (rapeseed oil versus SE powders) were first the absence of the band 3360 cm^{-1} in the oil, which would be expected since this peak was attributed to the O–H stretch of free hydroxyl, secondly a different profile in the band 900–1500 cm^{-1}, that is characteristic of the glycosidic band stretching for SE and thirdly a higher absorbance intensity in the band located around 740 cm^{-1} (C=O stretching). Despite these differences in the profiles of pure SE versus SE oleogel, when mixed in oil with a 1:9 (SE: oil) proportion, no matter the structuration used, the MIR spectra of the oleogels were very similar to pure oil. The only differences were found in *ethanol*-treated samples that showed an additional band around 880 cm^{-1}, a band 3360 cm^{-1}, and a slight change in the 900–1500 cm^{-1} region. Which might indicate that there is a small amount of ethanol left inside of the oleogel, or that there are more O–H connections between the SE treated with ethanol and the oil. A previous study of an extra virgin olive oil and SE without any *ethanol* treatment showed a band in 3100–4000 cm^{-1} in the infrared spectroscopy analysis pertaining to the stretching modes of –OH groups (Liu & Binks, 2021). The authors have attributed that band to the intermolecular H-bonds between TAG carbonyl groups and hydroxyl groups of trace impurity like fatty acid which confirms that in fact, ethanol improved the connections between the hydrophilic portion of the SE and the oil.

Published in : Food Chemistry (2023), vol. 405, Part B, 134927
DOI: 10.1016/j.foodchem.2022.134927
Status : Postprint (Author's version)

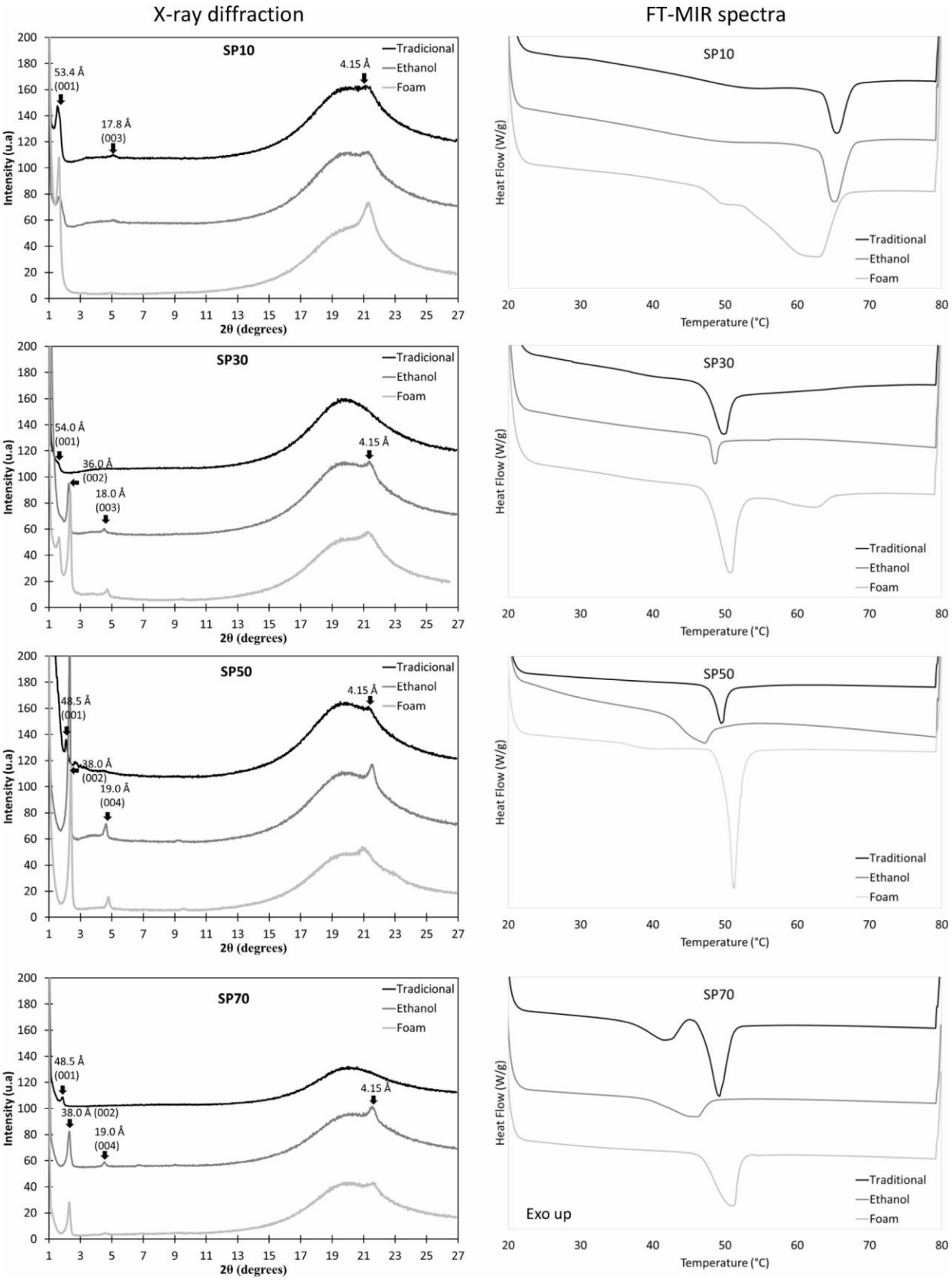

Fig. 5. X-ray diffraction (first column) and melting curves (second column) of the sucrose esters oleogels structured using different routes. Value indicated in Å in column 1 corresponds to d/n.

Published in : Food Chemistry (2023), vol. 405, Part B, 134927
DOI: 10.1016/j.foodchem.2022.134927
Status : Postprint (Author's version)

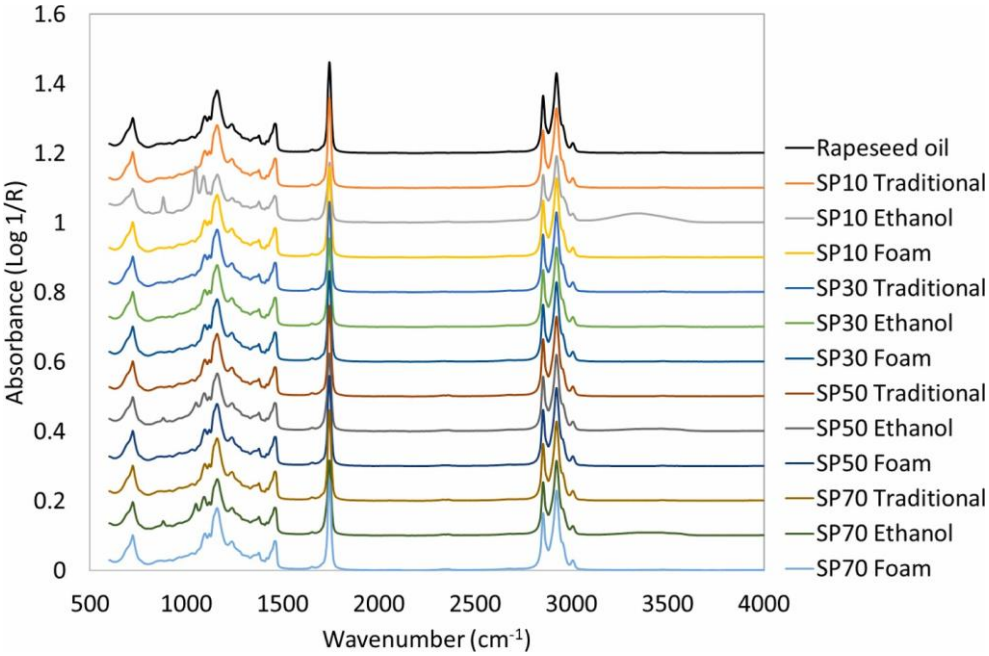

Fig. 6. FT-MIR spectra of the sucrose esters oleogels using different structuration routes.

Published in : Food Chemistry (2023), vol. 405, Part B, 134927
DOI: 10.1016/j.foodchem.2022.134927
Status : Postprint (Author's version)

Conclusion

Although the 4 investigated SE are not really promising oleogelators in low concentration using the *traditional* high-temperature route, they show a potential for oleogelation when alternative routes are used.

The best oleogel physical properties found in this study were with the SP50 *ethanol* (HLB 11). In SP50, even though it contained a high concentration of hydrophilic components – the monoesters –, the presence of ethanol during sample solubilization made it possible to solubilize it in oil with a good oil entrapment and mechanical properties. These results are attributed to the needle-like crystalline network formed, with more hydrogen bound connections between the oil and the SP50.

SP70 (HLB 15), although not leading to the best mechanical properties of the resulting oleogels, showed the best oil-binding capacity among all SEs and tested routes when the *foam*-template approach was used. In this sample, the previous dissolution in water followed by freeze-drying also improved the oil absorption/solubility of the SEs.

Although SP10 and SP30 were the most soluble in oils, they did not form a solid-like structure, regardless of the route tested. Based on these studies, to be able to obtain a better oleogel, with improved mechanical properties and 100 % oil binding capacity without increasing the amount of SE, an optimization of the oleogelation route should be explored or the combination of the SE treated with *foam*-template and *ethanol* with other oleogelators should be tested to find synergistic hybrid systems. Potentially hybrid systems could even allow to reduce the amount of SE, which would favour future food applications.

Declaration of Competing Interest

The authors declare that they have no known competing financial interests or personal relationships that could have appeared to influence the work reported in this paper.

Data availability

Data will be made available on request.

Acknowledgments

The authors are grateful for the Postdoctoral fellowships and funding in Sciences, Technology, Engineering, Materials, and Agrobiotechnology (STEMA) funding OTP N° DIVE.0899-J-P gave by ULiège

Published in : Food Chemistry (2023), vol. 405, Part B, 134927
DOI: 10.1016/j.foodchem.2022.134927
Status : Postprint (Author's version)

University Research Council. The authors also thanks Quentin Arnould from CRA-W for the support in the MIR analysis.

References

Abdollahi, M., Goli, S. A. H., & Soltanizadeh, N. (2020). Physicochemical properties of foam-templated oleogel based on gelatin and xanthan gum. *European Journal of Lipid Science and Technology, 122*(2), 1–9. https://doi.org/10.1002/ejlt.201900196

Blake, A. I., Co, E. D., & Marangoni, A. G. (2014). Structure and physical properties of plant wax crystal networks and their relationship to oil binding capacity. *Journal of the American Oil Chemists' Society, 91*(6), 885–903. https://doi.org/10.1007/s11746-014-2435-0

Blake, A. I., & Marangoni, A. G. (2015). The use of cooling rate to engineer the microstructure and oil binding capacity of wax crystal networks. *Food Biophysics, 10*, 456–465. https://doi.org/10.1007/s11483-015-9409-0

Chansanroj, K., & Betz, G. (2010). Sucrose esters with various hydrophilic-lipophilic properties: Novel controlled release agents for oral drug delivery matrix tablets prepared by direct compaction. *Acta Biomaterialia, 6*(8), 3101–3109. https://doi.org/10.1016/j.actbio.2010.01.044

Cheng, J., Kan, Q., Cao, J., Dudu, O. E., & Yan, T. (2021). Interfacial compositions of fat globules modulate coconut oil crystallization behavior and stability of whipped-frozen emulsions. *Food Hydrocolloids*, *114* (December 2020), 106580. https://doi.org/10.1016/j.foodhyd.2020.106580.

Co, E., & Marangoni, A. G. (2012). Organogels: An alternative edible oil-structuring method. *Journal of the American Oil Chemists' Society, 89*, 749–780. https://doi.org/10.1007/s11746-012-2049-3

da Silva, T. L. T., & Danthine, S. (2021). Effect of high-intensity ultrasound on the oleogelation and physical properties of high melting point monoglycerides and triglycerides oleogels. *Journal of Food Science, 86*(2), 343–356. https://doi.org/10.1111/1750-3841.15589

Doan, C. D., Davy, V. D. W., Patel, A. R., & Dewettinck, K. (2015). Evaluating the oil - Gelling properties of natural waxes in rice bran oil: Rheological, thermal, and microstructural study. *Journal of the American Oil Chemists' Society, 92*, 801–811. https://doi.org/10.1007/s11746-015-2645-0

Domingues, M. A. F., Da Silva, T. L. T., Ribeiro, A. P. B., Chiu, M. C., & Gonçalves, L. A. G. (2018). Structural characteristics of crystals formed in palm oil using sorbitan tristearate and sucrose stearate. *International Journal of Food Properties, 21*(1), 618–632. https://doi.org/10.1080/10942912.2018.1440237

Fayaz, G., Calligaris, S., & Nicoli, M. C. (2020). Comparative study on the ability of different oleogelators to structure sunflower oil. *Food Biophysics, 15*, 42–49. https:// doi.org/10.1007/s11483-019-09597-9

Fontenele Domingues, M. A., Badan Ribeiro, A. P., Chiu, M. C., & Gonçalves, L. A. G. (2015). Sorbitan and sucrose esters as modifiers of the solidification properties of zero trans fats. *LWT - Food Science and Technology, 62*(1), 122–130. https://doi.org/10.1016/j.lwt.2015.01.008

Garbolino, C., Bartoccini, M., & Flöter, E. (2005). The influence of emulsifiers on the crystallisation behaviour of a palm oil-based blend. *European Journal of Lipid Science and Technology, 107*(9), 616–626. https://doi.org/10.1002/ejlt.200501186

Garti, N., Clement, V., Leser, M., Aserin, A., & Fanun, M. (1999). Sucrose ester microemulsions. *Journal of Molecular Liquids, 80*(2–3), 253–296. https://doi.org/ 10.1016/s0167-7322(99)80010-5

Golodnizky, D., & Davidovich-Pinhas, M. (2020). The effect of the HLB value of sucrose ester on physiochemical properties of bigel systems. *Foods, 9*(12), 1–20. https://doi.org/10.3390/foods9121857

Guillen, M. D., & Cabo, N. (1997). Infrared spectroscopy in the study of edible oils and fats. *Journal of the Science of Food and Agriculture, 75*, 1–11. https://doi.org/10.1002/(SICI)1097-0010(199709)75:1<1::AID-JSFA842>3.0.CO;2-R

Husband, F. A., Sarney, D. B., Barnard, M. J., & Wilde, P. J. (1998). Comparison of foaming and interfacial properties of pure sucrose monolaurates, dilaurate and commercial preparations. *Food Hydrocolloids, 12*(2), 237–244. https://doi.org/10.1016/S0268-005X(98)00036-8

Jandacek, R. J., & Webb, M. R. (1978). Physical properties of pure sucrose octaesters. *Chemistry and Physics of Lipids, 22*, 163–176.

Kawaguchi, T., Hamanaka, T., Kito, Y., & Machida, H. (1991). Structural studies of a homologous series of alkyl sucrose ester micelle by X-ray scattering. *Journal of Physical Chemistry, 95*(9), 3837–3846. https://doi.org/10.1021/j100162a073

Kerr, R. M., Tombokan, X., Ghosh, S., & Martini, S. (2011). Crystallization behavior of anhydrous milk fat - sunflower oil wax blends. *Journal of Agricultural and Food Chemistry*, *59*, 2689–2695. https://doi.org/doi/abs/10.1021/jf1046046.

Kondamudi, N., & McDougal, O. M. (2019). Microwave-assisted synthesis and characterization of stearic acid sucrose ester: A bio-based surfactant. *Journal of Surfactants and Detergents, 22*(4), 721–729. https://doi.org/10.1002/jsde.12280

Liu, Y., & Binks, B. P. (2021). A novel strategy to fabricate stable oil foams with sucrose ester surfactant. *Journal of Colloid and Interface Science, 594*, 204–216. https://doi.org/10.1016/j.jcis.2021.03.021

Lopez, C., Lesieur, P., Bourgaux, C., & Ollivon, M. (2005). Thermal and structural behavior of anhydrous milk fat. 3. Influence of cooling rate. *Journal of Dairy Science, 88*(2), 511–526. https://doi.org/10.3168/jds.S0022-0302(05)72713-2

Lu, M., Cao, Y., Ho, C. T., & Huang, Q. (2016). Development of organogel-derived capsaicin nanoemulsion with improved bioaccessibility and reduced gastric mucosa irritation. *Journal of Agricultural and Food Chemistry, 64*(23), 4735–4741. https://doi.org/10.1021/acs.jafc.6b01095

Nelen, B. A. P., Bax, L., & Cooper, J. M. (2015). Sucrose esters. *Emulsifiers in Food Technology: Second Edition*, 147–180. https://doi.org/10.1002/9781118921265.ch7

Published in : Food Chemistry (2023), vol. 405, Part B, 134927
DOI: 10.1016/j.foodchem.2022.134927
Status : Postprint (Author's version)

Patel, A. R. (2017). Stable "arrested" non-aqueous edible foams based on food emulsifiers. *Food and Function, 8*(6), 2115–2120. https://doi.org/10.1039/c7fo00187h

Patel, A. R., & Dewettinck, K. (2015). Comparative evaluation of structured oil systems: Shellac oleogel, HPMC oleogel, and HIPE gel. *European Journal of Lipid Science and Technology, 117*(11), 1772–1781. https://doi.org/10.1002/ejlt.201400553

Patel, A. R., Schatteman, D., Lesaffer, A., & Dewettinck, K. (2013). A foam-templated approach for fabricating organogels using a water-soluble polymer. *RSC Advances, 3* (45), 22900–22903. https://doi.org/10.1039/c3ra44763d

Rincón-Cardona, J. A., Agudelo-Laverde, L. M., Martini, S., Candal, R. J., & Herrera, M. L. (2014). In situ synchrotron radiation X-ray scattering study on the effect of a stearic sucrose ester on polymorphic behavior of a new sunflower oil variety. *Food Research International, 64*, 9–17. https://doi.org/10.1016/j.foodres.2014.05.076

Rodriguez-Abreu, C., Aramaki, K., Tanaka, Y., Lopez-Quintela, M. A., Ishitobi, M., & Kunieda, H. (2005). Wormlike micelles and microemulsions in aqueous mixtures of sucrose esters and nonionic cosurfactants. *Journal of Colloid and Interface Science, 291* (2), 560–569. https://doi.org/10.1016/j.jcis.2005.05.018

Rodríguez-Negrette, A. C., Rodríguez-Batiller, M. J., García-Londoño, V. A., Borroni, V., Candal, R. J., & Herrera, M. L. (2021). Effect of sucrose esters on polymorphic behavior and crystallization kinetics of cupuassu fat and its fractions. *JAOCS, Journal of the American Oil Chemists' Society*, 1–15. https://doi.org/10.1002/aocs.12541

Sintang, M. D. B., Bin, S., Patel, A. R., Rimaux, T., Van De Walle, D., & Dewettinck, K. (2017). Mixed surfactant systems of sucrose esters and lecithin as a synergistic approach for oil structuring. *Journal of Colloid And Interface Science, 504*, 387–396. https://doi.org/10.1016/j.jcis.2017.05.114

Soultani, S., Ognier, S., Engasser, J. M., & Ghoul, M. (2003). Comparative study of some surface active properties of fructose esters and commercial sucrose esters. *Colloids and Surfaces A: Physicochemical and Engineering Aspects, 227*(1–3), 35–44. https://doi.org/10.1016/S0927-7757(03)00360-1

Szuts, A., Budai-Szucs, M., Eros, I., Ambrus, R., Otomo, N., & Szabó-Révész, P. (2010). Study of thermo-sensitive gel-forming properties of sucrose stearates. *Journal of Excipients and Food Chemicals, 1*(2), 13–20.

Szuts, A., Pallagi, E., Regdon, G., Aigner, Z., & Szabó-Révész, P. (2007). Study of thermal behaviour of sugar esters. *International Journal of Pharmaceutics, 336*(2), 199–207. https://doi.org/10.1016/j.ijpharm.2006.11.053

Szuts, A., & Szabó-Révész, P. (2012). Sucrose esters as natural surfactants in drug delivery systems—A mini-review. *International Journal of Pharmaceutics, 433*, 1–9. https://doi.org/10.1016/j.ijpharm.2012.04.076

Tangsanthatkun, J., & Sonwai, S. (2019). Crystallisation of palm olein under the influence of sucrose esters. *International Journal of Food Science and Technology, 54* (11), 3032–3041. https://doi.org/10.1111/ijfs.14216

Tavernier, I., Doan, C. D., Van de Walle, D., Danthine, S., Rimaux, T., & Dewettinck, K. (2017). Sequential crystallization of high and low melting waxes to improve oil structuring in wax-based oleogels. *The Royal Society of Chemistry, 7*, 12113–12125. https://doi.org/10.1039/C6RA27650D

Vieira, S. A., McClements, D. J., & Decker, E. A. (2015). Challenges of utilizing healthy fats in foods. *Advances in Nutrition, 6*, 309S–317S. https://doi.org/10.3945/an.114.006965

Watanabe, T., Kawai, T., & Nonomura, Y. (2018). Effects of fatty acid addition to oil-in- water emulsions stabilized with sucrose fatty acid ester. *Journal of Oleo Science, 67* (3), 307–313. https://doi.org/10.5650/jos.ess17097

Willett, S. A., & Akoh, C. C. (2019). Physicochemical characterization of organogels prepared from menhaden oil or structured lipid with phytosterol blend or sucrose stearate/ascorbyl palmitate blend. *Food and Function, 10*(1), 180–190. https://doi.org/10.1039/c8fo01725e

Ye, R., & Hayes, D. G. (2014). Recent progress for lipase-catalysed synthesis of sugar fatty acid esters. *Journal of Oil Palm Research, 26*(4), 355–365.

Youan, B. B. C., Hussain, A., & Nguyen, N. T. (2003). Evaluation of sucrose esters as alternative surfactants in microencapsulation of proteins by the solvent evaporation method. *AAPS Journal, 5*(2), 1–9.

Zeng, D., Cai, Y., Liu, T., Huang, L., Zeng, Y., Zhao, Q., & Zhao, M. (2021). The effect of sucrose esters S1570 on partial coalescence and whipping properties. *Food Hydrocolloids*, *125*(September 2021), 107429. https://doi.org/10.1016/j.foodhyd.2021.107429.